Organic LETTERS

Letter

pubs.acs.org/OrgLett

A Macrocyclization of 1,8-Bis(dithiafulvenyl)pyrenes

Mohammadreza Khadem, Joshua C. Walsh, Graham J. Bodwell,* and Yuming Zhao*

Department of Chemistry, Memorial University, St. John's, NL, Canada, A1B 3X7

Supporting Information

ABSTRACT: Dithiafulvenyl (DTF) end groups were linked to the 1 and 8 positions of a pyrene core directly or via phenylene bridges to afford redox-active pyrene derivatives. Upon oxidation, the 1,8-bis(DTF)pyrene underwent stepwise electron transfers to form radical cation and dication species, whereas the phenylene-extended bis(DTF)pyrene derivative was cyclized into a macrocyclic trimer through sequential DTF oxidative coupling reactions in solution and in the solid state. The structural, electronic, and supramolecular properties of the pyrene-based macrocycle were investigated using various spectroscopic techniques and molecular modeling studies.

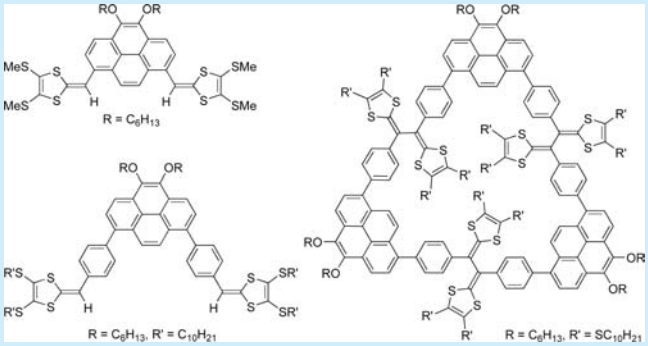

Pyrene has been widely used as a functional molecular building block for various π-conjugated nanomaterials and devices.[1] Linear and cyclic oligomers and polymers[2,3] can be readily synthesized by coupling disubstituted pyrenes with suitable divalent π-counterparts, whereby the substitution pattern of the pyrene unit plays an important role in determining the structures and properties of the resulting macromolecular systems. In our recent studies, the 1,8-pyrenylene motif was successfully exploited in constructing conjugated polymers[2b] and shape-persistent macrocycles[3a] through transition-metal-catalyzed cross-coupling reactions.

Other types of direct C−C bond-forming methods could also be useful in the preparation of functional pyrene-based materials and therefore warrant exploration. One such reaction is the oxidative coupling of dithiafulvenyl (DTF) units to afford tetrathiafulvalene vinylogues (TTFVs) (Scheme 1).[4] This reaction has been investigated actively in recent years as a synthetic tool for generating a broad range of redox-active and conformationally switchable π-systems and devices.[5]

In general, DTF-π-DTF systems **I** would be expected to yield extended oligo-/polymers **II** when subjected to oxidative coupling (Scheme 1). Although the possbility exists that cyclized products could also be generated, this is typically not the case.[6] Indeed, there is no precedent for direct macrocyclization from a DTF-π-DTF system **I** and only one clear example of macrocyclization through DTF oxidative coupling of oligomeric systems **II**, which afforded a mixture of cyclic products in low yields that were difficult to purify.[6a] Consequently, we became interested in the development of effective approaches to TTFV-containing macrocycles and we report herein the first successful macrocyclization via oxidative DTF coupling.

Scheme 1. General Mechanism for Oxidative DTF Coupling and Polymerization of Bis(DTF)-End-Capped Arenes

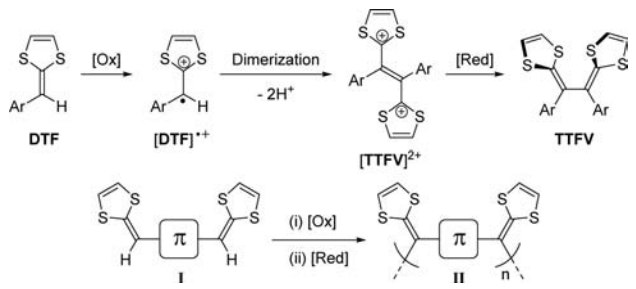

Pyrene derivatives with DTF units attached to the 1 and 8 positions were identified as suitable macrocyclization precursors due to their their wedge-like molecular shapes (*ortho*-phenylene-like geometry) and potential for strong intermolecular aggregation. Intital work was centered on 1,8-bis(DTF)-pyrene **4** (Scheme 2), which was synthesized from dibromide **1** in two steps via a lithiation−formylation reaction (88%) and then a phosphite-promoted olefination reaction (85%).[5a,6b,7] With the angular orientation (120° turn) of the two DTF groups and the rigid pyrenylene core, one can easily envision that oligomers arising from oxidative coupling of **4** could favor a folded conformation[2b] as the chain length grows. When the folded oligomer chain arrives at a full turn (trimer: 3 × 120° = 360°), cyclization might become favored.

Unfortunately, bis(DTF)pyrene **4** was found to be persistently unreactive toward oxidative coupling using a variety of oxidants (I_2, DDQ, CAN, $AgNO_3$, Ag_2O, $CuSO_4$, $FeCl_3$, $HgCl_2$, and $MoCl_5$) in CH_2Cl_2. Grinding neat **4** with excess iodine chips using a mortar and pestle for *ca.* 1 h was also tried, but this only ended up with nearly quantitative recovery of unreacted **4** after a reductive workup with aq. $Na_2S_2O_3$. Alternatively, slow diffusion of iodine vapor into a CH_2Cl_2

Received: March 28, 2016
Published: May 10, 2016

DOI: 10.1021/acs.orglett.6b00894
Org. Lett. 2016, 18, 2403−2406

Scheme 2. Synthesis of Bis(DTF)pyrenes 4 and 8

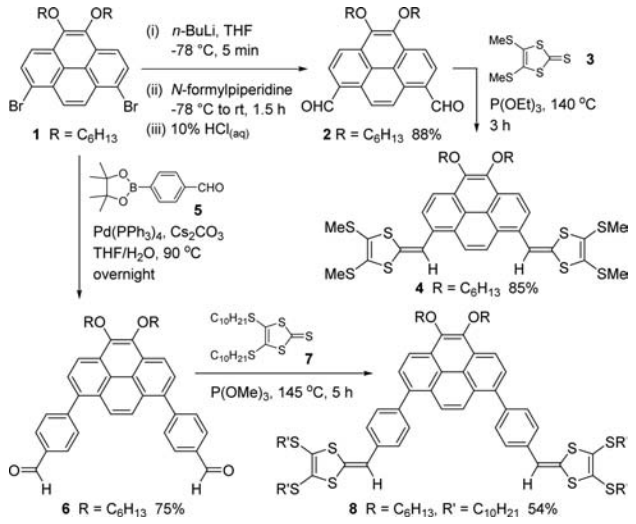

solution of **4** was performed, resulting in the formation of dark-colored crystalline needles, which may be charge-transfer salt(s).[8] X-ray single crystallographic analysis of one of the crystals failed to give meaningful results. Some orange crystals were found to coexist among the dark crystals, and a single crystal X-ray structure determination showed them to be neutral **4** (Figure 1A). In the crystal structure of **4**, the two

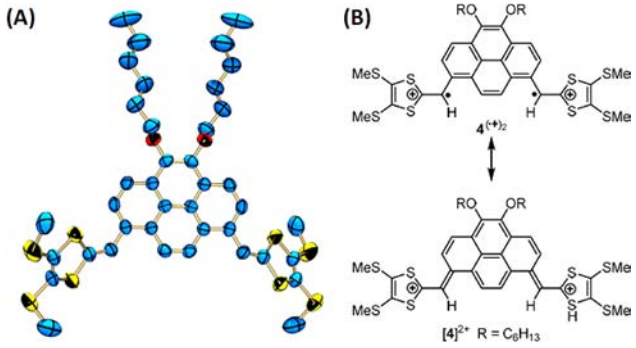

Figure 1. (A) ORTEP plot of compound **4** at 50% ellipsoid probability (CCDC#1450007). (B) Resonance structures for the singlet dication of **4**.

DTF groups form torsion angles of *ca.* 42° relative to the central pyrene unit. Such an orientation is in line with those observed in the single crystal structures of phenyl-substituted DTFs.[9] The moderate deviation from planarity in the DTF-pyrene-DTF skeleton suggests that π-delocalization is retained to a certain exent.

The unsuccessful oxidative coupling of **4** can be understood by consideration of its cyclic voltammetric (CV) data. The oxidation of **4** proceeds through two prominent anodic peaks at +0.57 V and +0.72 V (Figure 2A), which are assigned to sequential single-electron transfers in the two DTF groups. These oxidation potentials are considerably lower than those of typical arene-DTF derivatives (*ca.* +0.9 V to +1.1 V),[4−6,9] which can be attributed to an increasing degree of π-electron delocalization between the pyrene system in **4** and the two DTF units as they are oxidized. This is supported by UV−vis absorption analysis (Figure S23) and density functional theory (DFT) calculations,[10] which show that the DTF/pyrene

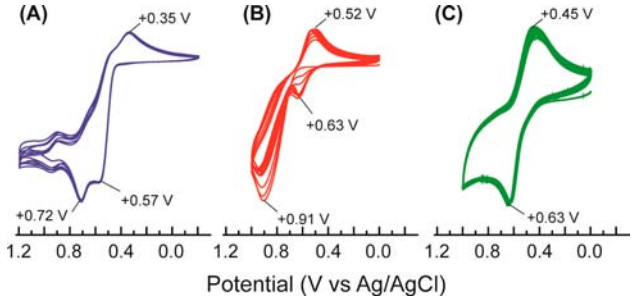

Figure 2. Cyclic voltammograms of (A) bis(DTF)pyrene **4**, (B) bis(DTF)pyrene **8**, and (C) macrocycle **10**. Solvent: CH_2Cl_2. Electrolyte: Bu_4NBF_4 (0.1 M). Working electrode: glassy carbon. Reference electrode: Ag/AgCl (3 M NaCl). Counter electrode: Pt. Scan rate: 0.3 V/s.

torsion angles in **4** decrease from 35.4° (neutral) to 18.6° (radical cation) and 4.3° (singlet dication) upon oxidation (Figures S15−S17). The triplet dication of **4** (Figure S18) was calculated to be 8.02 kcal/mol higher in energy than the singlet form, which the calculations showed to be best represented by the dication $\mathbf{4}^{2+}$ resonance structure (unreactive toward oxidative coupling) rather than bis(radical cation) $\mathbf{4}^{(\bullet+)2}$ (Figure 1B). Even the radical cation $\mathbf{4}^{\bullet+}$ was calculated to show very little spin density on the benzylic carbons (Figure S16), which is also consistent with the low reactivity toward oxidative coupling at this stage. This was corroborated experimentally by the multicycle CV scanning, where the CV profile of **4** remained nearly unchanged.

To circumvent the problems encountered with **4**, a modified bis(DTF)pyrene precursor **8** was designed (Scheme 2). Compound **8** differs from **4** in that a 1,4-phenylene unit has been inserted between each of the two DTF groups and the central pyrene core. This was intended to revive the DTF reactivity by reducing the electronic communication between the DTF units and the pyrene system.[6b] The synthesis of **8** began with a 2-fold Suzuki−Miyaura coupling between 1,8-dibromopyrene **1** and boronate **5**, which yielded dialdehyde **6** (75%). Compound **6** was then converted into bis(DTF)pyrene **8** via the phosphite-mediated olefination reaction.[5a,6b,7] CV analysis of **8** confirmed that the DTF groups were indeed reactivated. The first cycle of the anodic scan showed only one oxidation peak at +0.91 V, due to simultaneous electron transfers at the two DTF groups (Figure 2B).[4−6,9] In the case of the second cycle of CV scans, a new oxidation peak emerged, which offers clear evidence for the DTF groups undergoing the oxidative coupling on the surface of the working electrode.[4]

Iodine-induced oxidative coupling of bis(DTF)pyrene **8** was then performed in a CH_2Cl_2 solution (Conditions A, Scheme 3),[11] but the reaction was sluggish. After 1 h, the reaction mixture was found to consist of roughly equal amouts of dimerized product **9** and unreacted starting material **8** along with a small amount of a trimeric product (indicated by tlc, NMR, and especially MALDI-TOF MS analyses). When the reaction time was prolonged, higher oligomeric products were detected by MS analysis. Based on these results, it was concluded that solution phase conditions were unsuitable for macrocyclization.

Alternatively, solid-state conditions were investigated. Direct grinding of **8** with excess iodine using a mortar and pestle for 1 h led to the formation of a mixture of dimer **9**, a trimeric product, and unreacted **8** in similar amounts (tlc and MALDI-

DOI: 10.1021/acs.orglett.6b00894
Org. Lett. 2016, 18, 2403−2406

Scheme 3. Oxidative Coupling Reactions of Bis(DTF)pyrene 8 under Different Conditions

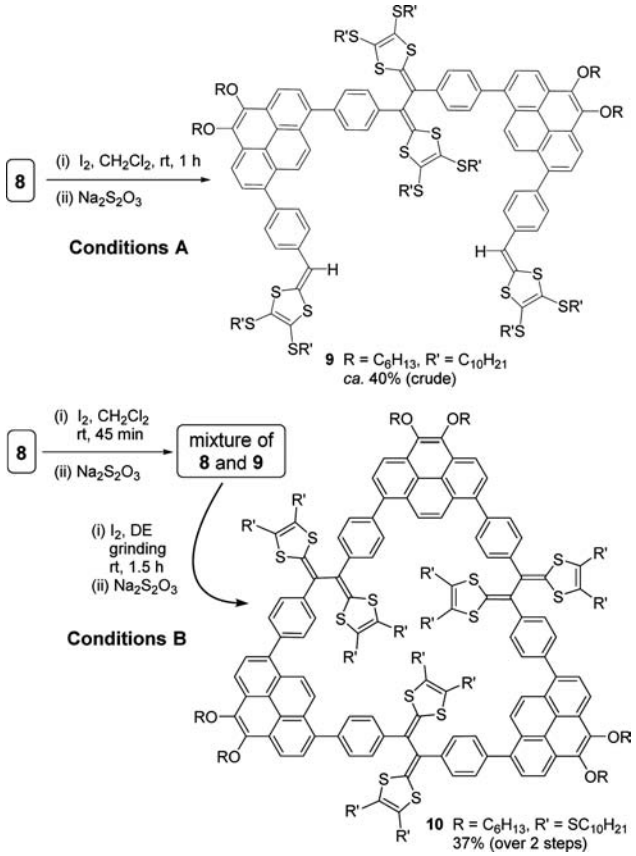

TOF MS analyses). Attempts to isolate the trimeric product in pure form by silica gel column chromatography were unsuccessful, so its stucture (whether linear or cyclic) could not be determined. Nevertheless, the solid-state conditions seemed to induce more effective DTF coupling than solution conditions.

The addition of grinding aids such as diatomaceous earth (DE) or silica gel was investigated as a means to increase the ease and efficiency of grinding. After numerous trials, a satisfactory two-step method for the synthesis of trimeric macrocyle **10** was established (Scheme 3). This method involves initial reaction of compound bis(DTF)pyrene **8** with iodine in CH_2Cl_2 for 45 min. Workup of this reaction yielded a solid mixture of roughly amounts of **8** and **9** (TLC analysis). Subjection of this mixture to grinding with iodine in the presence of DE for 1.5 h then furnished macrocycle **10** in 37% yield after preparative TLC. It appears that premixing monomer **8** and dimer **9** in the solid state is key to the success of the macrocyclization. Semiempirical modeling suggested that **8** and **9** can form a 1:1 aggregate through complementary π-stacking (Figure 3), whereby they are preorganized to favor a [1 + 1] macrocyclization.

Compound **10** was characterized by NMR, IR, and MALDI-TOF MS analyses, with the former and latter clearly supporting its cyclic trimeric nature.[10] The electrochemical redox properties of **10** were examined by CV analysis (Figure 2C) and oxidative UV–vis titration (Figure S20). A quasi-reversible redox wave pair (E_{pa} = +0.63 V, E_{pc} = +0.45 V) characteristic of typical TTFV redox behavior[4−6] was observed in the CV of **10**. The absence of a DTF oxidation peak (*cf.* voltammograms of **4**

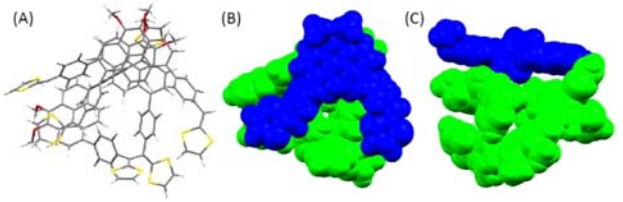

Figure 3. Molecular structure of a 1:1 aggregate of **8** and **9** optimized at the semiempirical RM1 level (Spartan'10). (A) Top view of the capped-stick model. Space-filling models showing (B) top and (C) side view. Color scheme: blue = **8**, green = **9**. $SC_{10}H_{21}$ groups were replaced with hydrogen atoms and OC_6H_{13} groups with OCH_3 groups to save computational expense.

and **8**) corroborated the macrocyclic structure of **10**. Molecular mechanics (MM) simulations indicated that macrocycle **10** can adopt a range of twisted, nonsymmetrical conformations. The simplicity of the aromatic region of the ^{1}H NMR spectrum of **10** (Figure 4A) points to rapid interconversion of conformers

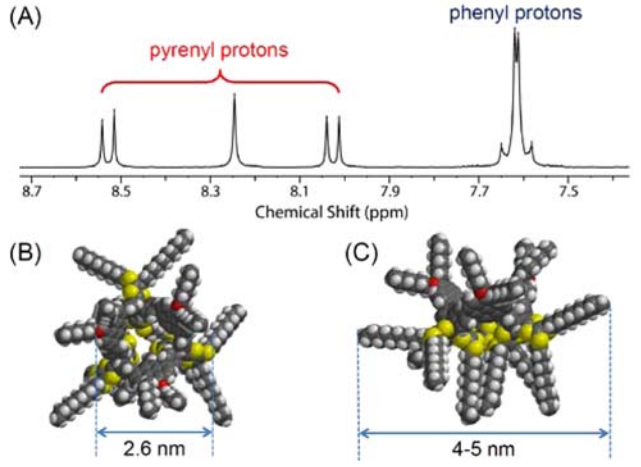

Figure 4. (A) Aromatic region of the ^{1}H NMR (500 MHz, $CDCl_3$) spectrum of **10**. (B) Top and (C) side views of the optimized geometry of **10** using the *MMFF* force field.

at room temperature, which averages to a threefold-symmetric structure. Pulsed gradient spin–echo (PGSE) NMR analysis of **10** gave an average diffusion coefficient (D) of 3.07×10^{-10} m^2 s^{-1} (based on the aromatic proton signals), which corresponds to a hydrodynamic diameter of 2.76 nm. This value is in good agreement with the calculated dimensions of the π-conjugated framework of **10** excluding the flexible alkyl chains (Figure 4B).

The modeling results also suggest that macrocycle **10** has an inner cavity large enough to host C_{60} fullerene; however, no significant binding was observed experimentally. It may be that the 18 alkyl chains on the periphery of **10** block the entry of the relatively large guest molecule to the central cavity. Upon moving to nitrobenzene, a much smaller guest molecule than C_{60}, macrocycle **10** was found to form a 1:1 complex. The binding constant (K_{assoc}) determined from a UV–vis titration experiment is 3644.6 ± 0.4 M^{-1} (Figure S19). The major driving force for the binding can be ascribed to π-stacking between pyrene and nitrobenzene.[2e]

In summary, we have developed a relatively effective two-stage synthetic method for the synthesis of a novel redox-active pyrene-TTFV macrocycle **10**, which involves sequential oxidative DTF coupling reactions in solution and the solid

DOI: 10.1021/acs.orglett.6b00894
Org. Lett. 2016, 18, 2403–2406

state. The success of this unique macrocyclization strategy can be explained by two key factors: (1) the solution-phase oxidative coupling of bis(DTF)pyrene **8** is sluggish and yields only a mixture of the dimer and unreacted monomer; (2) modeling suggests that the monomer and dimer favor complementary π-stacking in the solid state. The TTFV-pyrene macrocycle **10** and its bis(DTF)pyrene precursor **9** contribute useful building blocks for the preparation of redox-active supramolecular systems and functional molecular devices.

■ ASSOCIATED CONTENT

Supporting Information

The Supporting Information is available free of charge on the ACS Publications website at DOI: 10.1021/acs.orglett.6b00894.

Synthetic procedures and details of spectroscopic characterizations and molecular modeling studies(PDF)
Diffusion analysis details (PDF)
Crystallographic data for **4** (CIF)

■ AUTHOR INFORMATION

Corresponding Authors

*E-mail: gbodwell@mun.ca.
*E-mail: yuming@mun.ca.

Notes

The authors declare no competing financial interest.

■ ACKNOWLEDGMENTS

The authors acknowledge the Natural Sciences and Engineering Research Council of Canada (NSERC), Canada Foundation for Innovation (CFI), and Memorial University for financial support. Prof. Michael Katz of Memorial University is acknowledged for assistance in the X-ray crystallographic analysis.

■ REFERENCES

(1) (a) Figueira-Duarte, T. M.; Müllen, K. *Chem. Rev.* **2011**, *111*, 7260. (b) Duhamel, J. *Langmuir* **2012**, *28*, 6527. (c) Mateo-Alonso, A. *Chem. Soc. Rev.* **2014**, *43*, 6311. (d) Ghasemabadi, P. G.; Yao, T.; Bodwell, G. J. *Chem. Soc. Rev.* **2015**, *44*, 6494.

(2) For recent examples of pyrene-based conjugated polymers, see: (a) Bheemireddy, S. R.; Plunkett, K. N. *Polym. Chem.* **2016**, *7*, 292. (b) Younes, E. A.; Williams, K.-L. M.; Walsh, J. C.; Schneider, C. M.; Bodwell, G. J.; Zhao, Y. *RSC Adv.* **2015**, *5*, 23952. (c) Zhu, X.; Wu, Y.; Zhou, L.; Wang, Y.; Zhao, H.; Gao, B.; Ba, X. *Chin. J. Chem.* **2015**, *33*, 431. (d) Yang, D. S.; Kim, K. H.; Cho, M. J.; Jin, J.-I.; Choi, D. H. *J. Polym. Sci., Part A: Polym. Chem.* **2013**, *51*, 1457. (e) He, G.; Yan, N.; Yang, J.; Wang, H.; Ding, L.; Yin, S.; Fang, Y. *Macromolecules* **2011**, *44*, 4759. (f) Kawano, S.-i.; Yang, C.; Ribas, M.; Baluschev, S.; Baumgarten, M.; Müllen, K. *Macromolecules* **2008**, *41*, 7933.

(3) For recent examples of pyrene-based conjugated macrocycles, see: (a) Venkataramana, G.; Dongare, P.; Dawe, L. N.; Thompson, D. W.; Zhao, Y.; Bodwell, G. J. *Org. Lett.* **2011**, *13*, 2240. (b) Lorbach, D.; Keerthi, A.; Figueira-Duarte, T. M.; Baumgarten, M.; Wagner, M.; Müllen, K. *Angew. Chem. Int. Ed.* **2016**, *55*, 418. (c) López-Moreno, A.; Pérez, E. M. *Chem. Commun.* **2015**, *51*, 5421. (d) Iwamoto, T.; Kayahara, E.; Yasuda, N.; Suzuki, T.; Yamago, S. *Angew. Chem. Int. Ed.* **2014**, *53*, 6430. (e) Fujitsuka, M.; Tojo, S.; Iwamoto, T.; Kayahara, E.; Yamago, S.; Majima, T. *J. Phys. Chem. A* **2015**, *119*, 4136.

(4) (a) Lorcy, D.; Carlier, R.; Robert, A.; Tallec, A.; Le Magueres, P.; Ouahab, L. *J. Org. Chem.* **1995**, *60*, 2443. (b) Hapiot, P.; Lorcy, D.; Tallec, A.; Carlier, R.; Robert, A. *J. Phys. Chem.* **1996**, *100*, 14823.

(5) (a) Zhao, Y.; Chen, G.; Mulla, K.; Mahmud, I.; Liang, S.; Dongare, P.; Thompson, D. W.; Dawe, L. N.; Bouzan, S. *Pure Appl. Chem.* **2012**, *84*, 1005. (b) Bendikov, M.; Wudl, F.; Perepichka, D. F. *Chem. Rev.* **2004**, *104*, 4891. (c) Roncali, J. *J. Mater. Chem.* **1997**, *7*, 2307.

(6) (a) Bellec, N.; Boubekeur, K.; Carlier, R.; Hapiot, P.; Lorcy, D.; Tallec, A. *J. Phys. Chem. A* **2000**, *104*, 9750. (b) Khadem, M.; Zhao, Y. *J. Org. Chem.* **2015**, *80*, 7419.

(7) (a) Christensen, C. A.; Batsanov, A. S.; Bryce, M. R. *J. Org. Chem.* **2007**, *72*, 1301. (b) Schou, S. S.; Parker, C. R.; Lincke, K.; Jennum, K.; Vibenholt, J.; Kadziola, A.; Nielsen, M. B. *Synlett* **2013**, *24*, 231.

(8) (a) Naka, K.; Uemura, T.; Chujo, Y. *Polym. J.* **2000**, *32*, 435. (b) Gelover-Santiago, A.; Naka, K.; Chujo, Y. *J. Polym. Sci., Part A: Polym. Chem.* **2005**, *43*, 6592.

(9) Woolridge, K.; Goncalves, L. C.; Bouzan, S.; Chen, G.; Zhao, Y. *Tetrahedron Lett.* **2014**, *55*, 6362.

(10) See the Supporting Information for details.

(11) (a) Wang, Y.; Zhao, Y. *Org. Biomol. Chem.* **2015**, *13*, 9575. (b) Chen, G.; Mahmud, I.; Dawe, L. N.; Daniels, L. M.; Zhao, Y. *J. Org. Chem.* **2011**, *76*, 2701. (c) Chen, G.; Mahmud, I.; Dawe, L. N.; Zhao, Y. *Org. Lett.* **2010**, *12*, 704.

DOI: 10.1021/acs.orglett.6b00894
Org. Lett. 2016, 18, 2403−2406